Solid Freeform Fabrication 2022: Proceedings of the 33rd Annual International Solid Freeform Fabrication Symposium – An Additive Manufacturing Conference
Reviewed Paper

The Impact of the Printed Part Geometry on the Shrinkage and the Density of 316L Stainless Steel Parts Printed by FFF/FDM Technology

Suleiman Obeidat*, Joe Nervis Jr., Junkun Ma

Department of Engineering Technology, Sam Houston State University

*Corresponding author: obeidat@shsu.edu

Abstract

Additive manufacturing has been used extensively for the last decade in making different parts of different complexities. One of the additive manufacturing methods discussed in this work is Fused Filament Fabrication/ Fused Deposition Modeling (FFF/FDM). FDM is used to fabricate stainless steel using BASF Ultrafuse 316L Metal 3D printing filament which is made of 80 w. % 316L stainless steel particles in polymer base. We study the impact of the part geometry on the part shrinkage, apparent and relative density of 3D printed parts (green and sintered parts). Four basic geometries are printed: rectangular blocks, cylinders, spheres, and cones. These geometries have the same volume with the same height in the printing direction for the cylinders, rectangular blocks, and the cones. It is found that the relative density (apparent density/theoretical density) of approximately 99.0 % is achieved in the rectangular block compared to approximately 96.65 % for the cylinder, 98.0 % for the cone, and 95.8 % for the sphere. The highest shrinkage of 47.9 % takes place in the cylinder while the shrinkage in the rectangular block is approximately 44.42 % as a maximum.

Keywords: Additive manufacturing; FFF/ FDM; 316L stainless steel.

Introduction

Additive manufacturing is one of the operations used to make parts layer by layer instead of cutting materials to shape the part made as in the machining processes. In the last two decades, the industry has been using the additive manufacturing extensively in making complicated parts that can be used in different applications such as biomedical implants, heat engines and other applications that need complicated and strong parts with intricate details. But as any other manufacturing processes, making fully defect free parts is not possible. These defects such as pores and cracks in the printed part impact the mechanical properties of the part. These pores and cracks come from the way the part is manufactured, the manufacturing process parameters and the complexity of the part which include its shape. Different researchers studied different factors that affect the mechanical properties of the parts printed. [1] Liu et al. (2020) and [2] Gong et al. (2019) compared between the parts made by FDM and those ones made by Selective Laser Melting process. [1] stated that FDM technology followed by de-binding and sintering is a more energy-saving process to fabricate metal parts compared to Selective Laser Melting process. They used the FDM technology to produce 316L stainless steel and they concluded that the parts made using FDM are weaker than the parts made using Selective Laser Melting but at the same time they stated that denser products can be made with different printing parameters and improved sintering process.[3] Schumacher and Moritzer (2021) used FDM technology and the BASF 3D Printing

Solutions GmbH material Ultrafuse 316L to make metallic parts. They studied the effect of material specific FDM processing parameters on the properties of the sintered parts (white parts). They used the density of the green parts produced as an evaluation criterion to assess the white part quality. [4] Abe et al. (2021) studied the effect of layer directions on internal structures and tensile properties of 17-4PH stainless steel parts fabricated by FDM. They found that the as sintered specimens printed with its direction perpendicular to the tensile direction achieved the highest ultimate strength. Also, they found that the linear shrinkage is higher in the printing direction than in the other directions. [5] Wang et al. (2019) studied the effect of raster orientation and extrusion width in the FDM process on the porosity and mechanical behavior of 3D printed parts. They used X-ray computed tomography (XCT) to characterize the pores inside the printed structure to predict the mechanical properties of the parts printed. [6] Quarto et al. (2021) used Analysis of Variance to study the effect of different printing parameters on the density, porosity and shrinkage of the 316L stainless steel parts printed using fused deposition modeling (FDM). [7] Patti et al. (2021) studied the thermo- mechanical properties and the effect of porosity on those properties of 316L stainless steel printed using FDM at different infill densities. [8] Hassan et al. (2021) investigated the microstructure and the mechanical properties of the 316L stainless steel at different values of part orientation, extrusion velocity and layer height. They found that there is a minor effect of the extrusion velocity and the layer thickness on the porosity and the grain size. [9] Tosto at al. (2021) studied the properties of Ultrafuse 316L BASF and 14-4 PH Makerforged printed using FDM. They investigated the mechanical properties of the printed parts and they related them with the raster bonding and the voids present in the green and sintered parts. [10] Rosnitschek et al. (2021) studied the effect of the part geometry and the infill degrees on the mechanical properties of 316L stainless steel fabricated by FDM. [11] Maconachie at al. (2020) confirmed that the mechanical behavior of the gyroids fabricated by fused deposition modeling is affected by the geometry and the topology of the gyroids rather than the manufacturing effects. They used in their study acrylonitrile butadiene styrene (ABS) to print those parts. [12] Moritzer et al. (2021) studied the effect of the strand geometry and nozzle size on the density of the green parts and the mechanical properties of the sintered 3D printed parts. Our objective is to study the effect of the geometry of the part fabricated using Fused Filament Fabrication/ Fused Deposition Modeling (FFF/ FDM) on the apparent and relative density and the shrinkage percentage of the sintered parts. We used the BASF Ultrafuse 316L Metal 3D printing filament which is made of 80 w. % 316L stainless steel particles in polymer base. It is up to the authors knowledge that this topic has not been studied in this way. General geometries such as rectangular bocks, cylinders, cones, and spheres are printed using (FFF/ FDM). BASF Ultrafuse 316L Metal 3D printing filaments are used to make these parts.

Materials and Methods: Parts Fabrication

The parts are made using (FFF/FDM) process using MakerBot Method X 3D printer. The process starts with creating a CAD model using a computer aided design (CAD) software then convert this file into (.stl) format which is compatible with these types of printers. The filament material we use is 316L Stainless steel powder of 80 w. % mixed with 20 w. % resin. Fig. 1 shows this printer. Filaments of 1.75 mm diameter have been used. The four basic shapes used are rectangular blocks, cylinders, spheres, and cones. The building plate is prepared by scraping any

residues from previous prints and then adding Magigoo Pro Metal 3D Bed Adhesion Solution for BASF Ultrafuse 316L. As shown in Fig. 1, this printer has two extruders; one of them is for building material which is 316L stainless steel, and the other is for support material. Here we did not use support material since we don't have over hanged parts and there is no possibility of bending the parts printed. We used one extruder of LABS extruder type which is used mainly for metals. The printing parameters used are all the same in all the prints to be consistent and to only investigate the effect of the part geometry on the shrinkage and the density of the part printed.

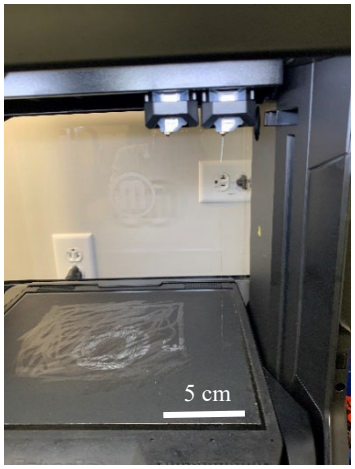

Fig. 1: Makerbot Method X 3D printer.

We printed 3 cylinders, 3 rectangular blocks, 3 spheres, and 3 cones. The parts built are created in a way that their volumes are the same in all the prints. A cylinder of 15 mm diameter and 20 mm height has been chosen to start with. The volume of this cylinder is 3534.3 mm^3. We chose the height to be the same for the cylinders, the cones, and the rectangular blocks and then we calculated the other dimensions based on a constant volume (3534.3 mm^3) and a height of 20 mm. The rectangular block is chosen to be of a square base. Table 1 shows the dimensions of the parts to be printed. After the fabrication process, the parts are de-bound and sintered to improve their mechanical properties. Some of the printing parameters used are layer thickness: 0.2 mm, extrusion temp.: 245 °C, chamber temp.: 85 °C, infill percentage: 100 %, infill pattern: linear, and the travel speed: 250 mm/s. All the parameters are the same in all samples.

Table 1: Dimensions of the parts printed.

Part	Volume (mm^3)	Height (mm)	Diameter (mm)	Width (mm)	Surface area (mm^2)
Rectangular block	3534.3	20	NA	13.29	1416.448
Cylinder	3534.3	20	15	NA	1295.25
Cone	3534.3	20	25.98	NA	1345.616
Sphere	3534.3	NA	18.9	NA	1121.639

Materials and Methods: De- Binding and Sintering Process

The samples were sent to DSH technologies, LLC for the thermal de-binding and sintering process. The green parts and the sintered ones are shown in Fig. 2.

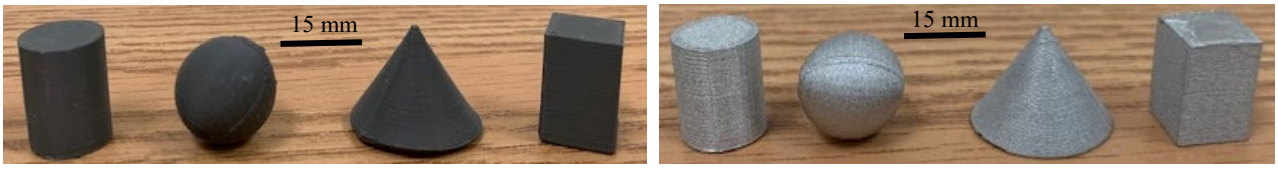

Fig. 2: 316L stainless steel printed green parts (left) and sintered parts (right).

The dimensions and the densities have been measured for the green parts and the sintered parts. Three samples have been printed and sintered of each geometry shown in Fig. 2. The dimensions have been measured using a regular caliper and the density has been measured using Archimedes method. Torbal AGCN220 Internal Calibration Analytical Balance, 220 g x 0.0001 g balance has been used in the process in addition to Torbal Density Kit for AGCN Scales.

Results and Discussion

As mentioned above the density has been measured using the Archimedes method. Apparent density has been calculated using equation 1 [13]. Fig. 3 shows the apparent density of the green parts. It shows that the rectangular block apparent density is higher than that of the cylinder which in turn is higher than that of the cone and the sphere.

$$\rho_a = \rho_{wt} \frac{m_d}{m_d - m_w} \quad (1)$$

ρ_a: Apparent density of the part.

ρ_{wt}: Water density at the measurement temperature

m_d: dry mass of the part

m_w: wet mass of the part

Fig. 4 shows the apparent density of the sintered parts. It is noticed that the sintered parts have almost the same trend as the green parts for some samples where the highest apparent density is for the rectangular block, then cylinder, sphere, and cone. In other samples, the cone or the cylinder have the highest apparent density. The apparent density of the rectangular block is the highest between them all. This might be because the rectangular blocks have the largest surface area as shown in table 1. Having a high surface area means that the rate of heat transfer is higher which makes the de-binding and the sintering process more efficient which in turn improves the part density. The surface areas of the cylinder and the cone are close to each other which explains why the apparent density of those two parts are close to each other. The surface area of the sphere is the smallest, but its apparent density is close to that of the cylinder in some samples. The bars shown in Fig. 4, Fig. 5, and Fig. 6 are the standard deviation of the measured values. From these

bars, it is concluded that more research is needed with different shapes, bigger size parts, and different printing parameters.

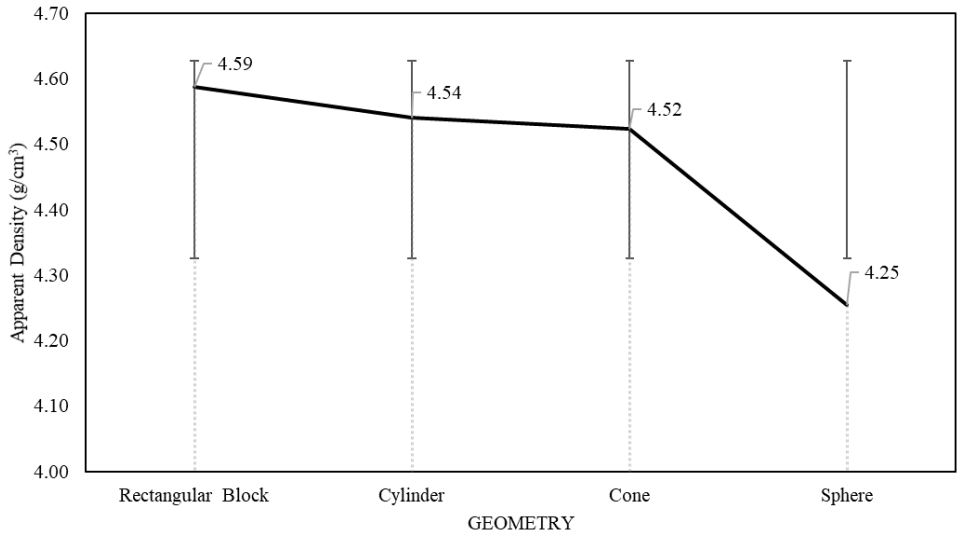

Fig. 3: Green parts apparent density

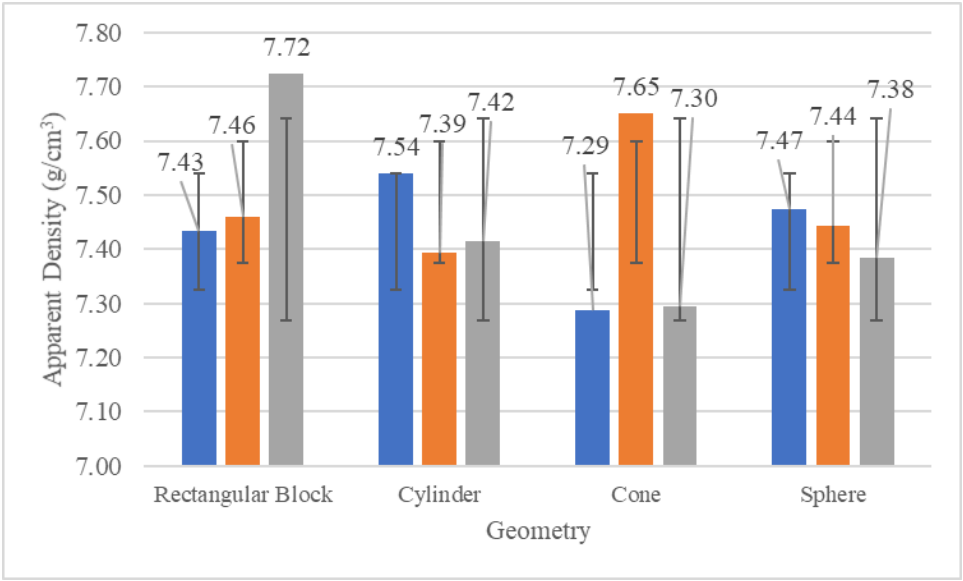

Fig. 4: Sintered parts apparent density

Fig. 5 shows the relative density (apparent density/theoretical density) of the 316L stainless steel. The theoretical density used here is 7.8 g/cm^3. Fig. 5 shows that a range of about 95.0 % to 99.0 % relative density in the rectangular block is achieved compared to a maximum of 96.65 % for the cylinder, about 98.0 % for the cone, and about 95.8 % for the sphere . This indicates again that a more relative density is achieved with higher surface area of the part printed but more investigation is needed with some other shapes and bigger volume parts. The shrinkage percentage has been measured, too. The volume of the sintered parts is compared with the volume of the green

parts. Fig. 6 shows the shrinkage percentages for the different shapes under study. It is noticed that the highest shrinkage takes place in the cylinder with 47.9 %, then the sphere with a maximum shrinkage of 46.63%, then cone with 45.77 %, and finally the rectangular block with a maximum of 44.42 %. This also is justified by the highest surface area of the rectangular block compared to the other geometries.

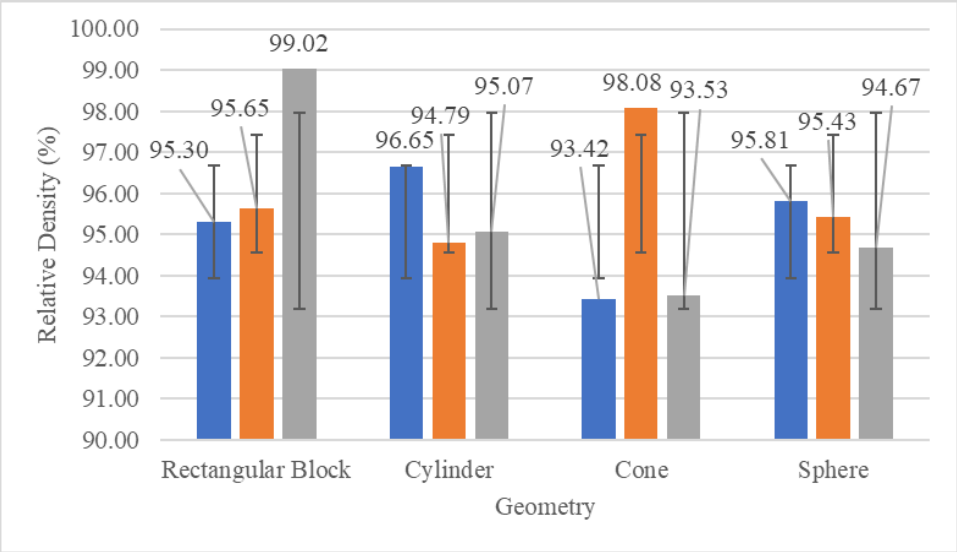

Fig. 5: Relative density of the 316L SS after sintering

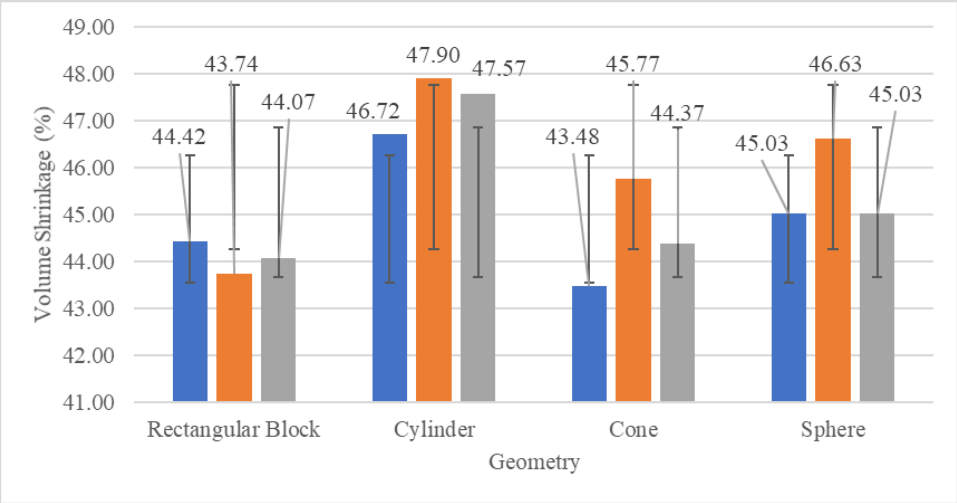

Fig. 6: Volume shrinkage of the sintered parts

Conclusions

FFF/ FDM technology is used to study the impact of the part geometry on the part shrinkage and the apparent density. 316L stainless steel parts at specific printing parameters are built in different shapes such as rectangular blocks, cylinders, cones, and spheres. The parts built are of the same volume but of different surface areas. We sintered the samples to obtain the metallic parts

of high density. Archimedes method is used to measure the apparent density of the green and sintered parts. Approximately 99.0 % relative density is achieved as a maximum in rectangular blocks while a 93.42 % is achieved in the cones as a minimum. The highest shrinkage of 47.9 % takes place in the cylinder while the shrinkage in the rectangular block is about 44.42 % as a maximum. One of the reasons for this result is the highest surface area of the rectangular blocks compared to the other geometries. Research is underway to investigate the impact of the raster angle, the overlap between the rasters, and to investigate different shapes and sizes on the relative density. It is expected that the overlap between the rasters would improve the relative density.

REFERENCES

[1] Liu, Bin; Wang, Yuxiang; Lin, Ziwei; Zhang, Tao, "Creating metal parts by Fused Deposition Modeling and Sintering", Materials Letters, Volume 263, 15 March 2020, 127252.

[2] Haijun, Gong; Snelling, Dean; Kamran, Kardel; and Carran, Andres, Comparison of Stainless Steel 316L Parts Made by FDM-and SLM-Based Additive Manufacturing Processes, JOM, Vol. 71, No. 3, 2019, https://doi.org/10.1007/sl1837-018-3207-3 © 2018 The Minerals, Metals & Materials Society.

[3] Schumacher, Christian; and Moritzer, Elmer, "Steel Parts Produced by Fused Deposition Modeling and a Sintering Process Compared to Components Manufactured in Selective Laser Melting", Macromolecular Symposia, Vol. 395 Issue 1, p1-4, 4p; DOI: 10.1002/masy.202000275 15 February 2021, https://doi- org.ezproxy.shsu.edu/10.1002/masy

[4] Abe, Yoshifumi; Kurose,Takashi; Santos, Marcelo V. A.; Kanaya, Yota; Ishigami, Akira; Shigeo Tanaka; and Ito,Hiroshi, " Effect of Layer Directions on Internal Structures and Tensile Properties of 17-4PH Stainless Steel Parts Fabricated by Fused Deposition of Metals,*Materials* 2021, *14*(2), 243; https://doi.org/10.3390/ma14020243.

[5] Wang X, Zhao L, Fuh JYH, Lee HP. Effect of Porosity on Mechanical Properties of 3D Printed Polymers: Experiments and Micromechanical Modeling Based on X-ray Computed Tomography Analysis. POLYMERS. 2019;11(7):1154. doi:10.3390/polym11071154.

[6] Quarto, M.; Carminati, M.; D'urso, G. Density and shrinkage evaluation of AISI 316L parts printed via FDM process. Materials & Manufacturing Processes, [s. l.], v. 36, n. 13, p. 1535–1543, 2021. DOI 10.1080/10426914.2021.1905830.

[7] Patti A, Cicala G, Tosto C, Saitta L, Acierno D. Characterization of 3D Printed Highly Filled Composite: Structure, Thermal Diffusivity and Dynamic-Mechanical Analysis. CET Journal-Chemical Engineering Transactions. 2021;86:1537-1542. doi:10.3303/CET2186257.

[8] Hassan W, Farid MA, Tosi A, Rane K, Strano M. The effect of printing parameters on sintered properties of extrusion-based additively manufactured stainless steel 316L parts. International Journal of Advanced Manufacturing Technology. 2021;114(9/10):3057-3067. doi:10.1007/s00170-021-07047-w.

[9] Tosto C, Tirillò J, Sarasini F, Cicala G. Hybrid Metal/Polymer Filaments for Fused Filament Fabrication (FFF) to Print Metal Parts. Applied Sciences (2076-3417). 2021;11(4):1444. doi:10.3390/app11041444.

[10] Rosnitschek T, Seefeldt A, Alber-Laukant B, Neumeyer T, Altstädt V, Tremmel S. Correlations of Geometry and Infill Degree of Extrusion Additively Manufactured 316L Stainless Steel Components. Materials (1996-1944). 2021;14(18):5173. doi:10.3390/ma14185173.

[11] Maconachie, T., Tino, R., Lozanovski, B., Watson, M., Jones, A., Pandelidi, C., Alghamdi, A., Almalki, A., Downing, D., Brandt, M., & Leary, M. (2020). The compressive behaviour of ABS gyroid lattice structures manufactured by fused deposition modelling. International Journal of Advanced Manufacturing Technology, 107(11/12), 4449–4467. https://doi-org.ezproxy.shsu.edu/10.1007/s00170-020-05239-4.

[12] Moritzer E, Elsner CL, Schumacher C. Investigation of metal-polymer composites manufactured by fused deposition modeling with regard to process parameters. Polymer Composites. 2021;42(11):6065. doi:10.1002/pc.26285.

[13] Diptanshu, Young E, Ma C, Obeidat S, Pang B, Kang N. Ceramic Additive Manufacturing Using VAT Photopolymerization. ASME international conference on manufacturing science and engineering. 2018;1:V001T01A003.